EARTH SURFACE PROCESSES AND LANDFORMS
*Earth Surf. Process. Landforms* **41**, 1467–1476 (2016)

Published online 23 February 2016 in Wiley Online Library
(wileyonlinelibrary.com) DOI: 10.1002/esp.3907

# OSL dating of past lake levels for a large dammed lake in southern Tibet and determination of possible controls on lake evolution

**Yiwei Chen,[1,2] Jonathan C. Aitchison,[3] Yongqiang Zong[2]* and Sheng-Hua Li[2]**
[1] State Key Laboratory of Isotope Geochemistry, Guangzhou Institute of Geochemistry, Chinese Academy of Sciences, Wushan, Tianhe District, Guangzhou, China
[2] Department of Earth Sciences, The University of Hong Kong, Hong Kong SAR, China
[3] School of Geography, Planning and Environmental Management, The University of Queensland, Brisbane, Queensland, Australia

Received 11 November 2014; Revised 3 January 2016; Accepted 18 January 2016

*Correspondence to: Yongqiang Zong, Department of Earth Sciences, The University of Hong Kong, Hong Kong SAR, China. E-mail: yqzong@hku.hk

ESPL
Earth Surface Processes and Landforms

ABSTRACT: Fluvio-lacustrine terraces along Phung Chu (river) on the central southern Tibetan Plateau indicate that a large palaeo-dammed-lake formerly existed in this area. Based on landscape survey, optically stimulated luminescence (OSL) dating and sedimentary analyses, this research shows that the Phung Chu was blocked and a dammed-lake over 2500 $km^2$ in size formed before 30 ka ago. OSL dating analysis suggests the fluvio-lacustrine sediments were well bleached and yield accurate age estimates for two lake drainage events. The first drainage event took place after 30 ka, resulted in river incision and formed a high terrace at 50 m height from the present river level. The second drainage happened after 3.7 ka, resulted in further river incision and formed the second terrace at 25 m height from the present river level. According to the distribution of the fluvio-lacustrine sediments, active normal faults (particularly the Kharta Fault) in this region and the high gradient slopes after Phung Chu enters the Yö Ri gorge, seismically-induced landsliding is regarded as highly likely to have been the cause of river blockage and associated formation of a dammed-lake, although glacial damming is also a possible cause. The volume of drainages from this dammed-lake may have led to catastrophic flooding and analogous modern lakes represent significant geo-hazard risks to down-river human settlements. As dammed-lakes are special phases in fluvial evolution, often involving river blockage, breakthrough and drastic catchment change, these processes can reveal how tectonic or climatic events modify landforms. However, such tectonic-derived landform changes can also impact palaeo-climate of the region. Thus this study has added new evidence regarding the evolutionary history of a dammed lake including its formation, duration, extent and final drainage, which is crucial for understanding its general landscape process mechanisms and for better assessing geo-hazard risks. Copyright © 2016 John Wiley & Sons, Ltd.

KEYWORDS: fluvio-lacustrine sediment; dammed lake; OSL dating; geo-hazard; Tibet

## Introduction

Dammed lakes commonly develop in areas of high topographic relief where they form as a result of river channel blockages that can be triggered by a variety of events. These include landslide and rock falls during seismic events, debris flows, glacial advances and moraine deposition (Keefer, 1984, 1994; Costa and Schuster, 1988; Korup *et al.*, 2006, 2010; Zhu *et al.*, 2013). The formation and drainage of such lakes has implications for studies of neotectonics (e.g. Chen *et al.*, 2013a), landscape evolutionary history (e.g. Korup and Montgomery, 2008), ice sheet advance (e.g. Mangerud *et al.*, 2001; Montgomery *et al.*, 2004) and geo-hazards (e.g. McColl, 2012; Yuan *et al.*, 2013). For instance, it has been reported that glacial damming of Tibetan rivers has important geomorphic consequences. This is because glacial stabilization of rivers impedes headward incision and thus helps maintain plateau topography (Korup and Montgomery, 2008).

Landslides have also long been studied using information from dammed lake sediments to reveal faulting activities and palaeo-seismic events in the late Quaternary (e.g. Costa and Schuster, 1991; Wang *et al.*, 2011; Nagelisen *et al.*, 2015). Dammed lakes may also provide key evidence that constrains aspects of the evolution of fluvial systems (e.g. Korup *et al.*, 2006). For instance, lacustrine sediments found in the upper reaches of the Yangtze River valley suggest the existence of a large dammed lake and subsequent down-cutting of the river; key evidence for the birth of the modern Yangtze River (Kong *et al.*, 2009). During catastrophic drainages of a large dammed lake, floods and extreme erosive events could rapidly change local geomorphology and sediment budgets, thus playing an important role in shaping the modern topography (e.g. Montgomery *et al.*, 2004; Dortch *et al.*, 2011).

Dammed lakes not only record landscape evolution, but are also a major secondary geo-hazard (e.g. Yin *et al.*, 2009; Hanson *et al.*, 2012). In large river valleys especially, the breaching of dammed lakes could lead to catastrophic loss of life (Dai *et al.*, 2005). The evolution of dammed-lakes including their formation, duration and breach provides key information for better assessing geological hazards for modern dammed lakes (e.g. Fan *et al.*, 2014; Scherler *et al.*, 2014). Moreover, environmental proxy studies like pollen records from lacustrine sediment are valuable materials for palaeo-climate reconstructions (e.g. Wang *et al.*, 2005).

Following the formation of dammed lakes, deposition of fluvio-lacustrine sediments commences. Because these lakes usually form in high relief river valleys, gullies or tributaries that used to join the river now begin to build out fans into the lake. During the 'high lake-period', relatively deep and stable water conditions provide a sedimentary environment that favors deposition of lacustrine sediments such as well-sorted fine silts. Coarser sediments like sand or gravel carried as bedload in tributaries tend to be deposited at gully mouths near the lakeshore to form delta-like sequences. With breaching of dams, lakes drain and disappear, sedimentary environments then return to fluvial conditions. Sediment accumulation during the lake-period is thus changed to fluvial incision, and in this case, fluvio-lacustrine sediments deposited during the 'high lake-period' could remain stranded as terraces along valley slopes high above the new riverbed. A series of such terraces and sediment associations therefore could provide useful evidence for the evolutionary history of dammed lakes including their formation, duration and drainage.

The Ama Drime massif, located in central southern Tibet, is a tectonic horst that provides an important window into deep crustal levels of the associated India-Asia orogenic system. This north–south (N–S) oriented range is bounded on either side by active normal faults, the Kharta Fault to the west and Dinggye Fault to the east (Armijo *et al.*, 1986; Leloup *et al.*, 2010). (Note that other researchers refer to these faults as the Ama Drime and Nyönno Ri detachments [Jessup *et al.*, 2008].) The massif protrudes north of the main east–west (E–W) trending Himalayan range. It offsets the South Tibet Detachment System (STDS), providing a minimum time bound for final displacement across this key > 1500 km long regional structure (e.g. Burchfiel *et al.*, 1992; Leloup *et al.*, 2010); that is related to evolution of the India-Asia orogenic system. It has been reported that normal faulting remains active today, but little is known about the late Quaternary tectonic activities for the Ama Drime range (e.g. Jessup *et al.*, 2008).

The deeply incised Yö Ri Gorge is part of the Arun River, one of the few drainages that bisects the Himalaya (Heron, 1922; Olen *et al.*, 2015). The existence of well-preserved fluvio-lacustrine sediments and terraces along the Phung Chu valley between the town of old Tingri and the Yö Ri Gorge (Figures 1 and 2) that clearly suggest river incision has long been known (e.g. Wager, 1937). However, their significance has never been addressed and several important questions await further resolution. When did these terraces form? How big was the dammed lake? What caused lake formation? Are there aspects of regional tectonic history that we can learn from these terraces? To answer these questions, we investigated a series of fluvio-lacustrine sediments along the Phung Chu valley between Tingri and the Yö Ri Gorge.

In this work we examined sediment samples collected from the terraces and determined when they formed using optically simulated luminescence (OSL) methods. Results of this study are used to infer an evolutionary history for the dammed lake. Possible controls for the lake drainage are discussed along with their implications for regional tectonic activities for one of the major normal faults in the central Himalaya, the Kharta Fault, which bounds the western margin of the Ama Drime Massif.

## Regional Setting

The Arun River, also known as Phung Chu in Tibet, originates from a glacier *c.* 6700 m above sea level (a.s.l.) on the northern slope of Shisha Pangma and flows eastwards. To the southeast

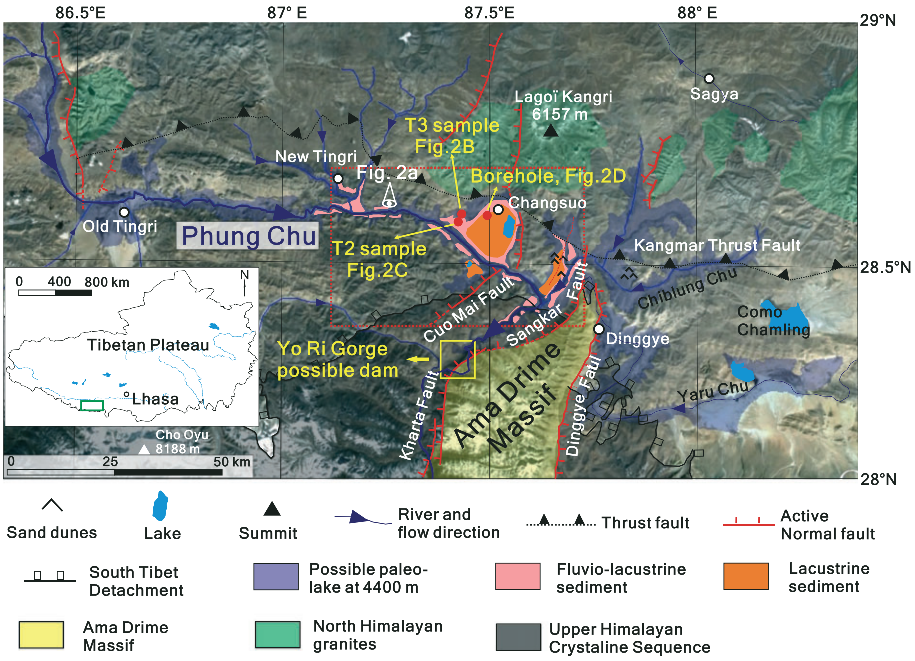


**Figure 1.** Structural geology and geomorphology of study region near Tingri (after Leloup *et al.*, 2010; base satellite imagery from Google Earth). The Ama Drime Massif (light yellow area) is bounded on both sides by active normal faults, Kharta Fault to the west and Dingye Fault to the east. Most rocks in the Ama Drime Range are comprised of migmatitic orthogneisses containing large layers and boudins of metabasites (Leloup *et al.*, 2010). Note the Yö Ri gorge (yellow rectangle in the lower-middle) before the abrupt turn of Phung Chu. Along the course of the river near Changsuo, the presence of fluvio-lacustrine (pink area) and lacustrine sediment (dark yellow area) high above the riverbed suggests a palaeolake once existed. The dark blue area represents the possible extent of the lake at a water level of 4400 m a.s.l., as reconstructed by DEM analysis from the Shuttle Radar Topography Mission (SRTM) data of ~90-m horizontal resolution. Note the locations of sampling sites and viewpoint.

 

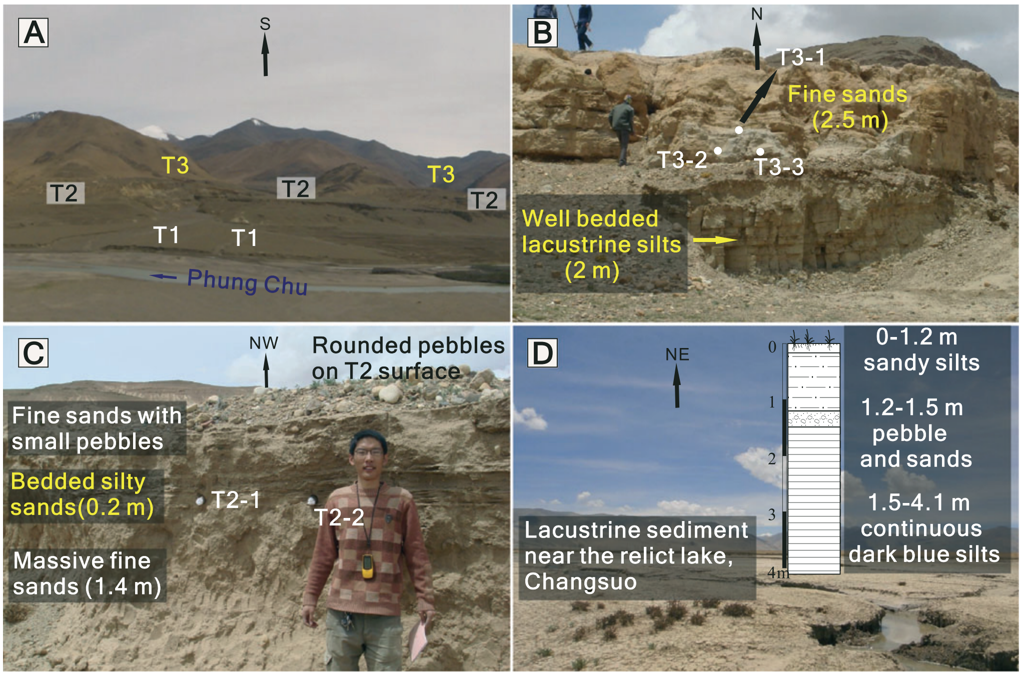


**Figure 2.** (A) An overview of the three terraces. T3 is *c.* 50 m above the riverbed, T2 is *c.* 25 m and T1 is *c.* 5 m. Note the viewpoint is shown on Figure 1. (B) and (C). Field photograph for profile A–A′ (note the location of A–A′ profile is shown in Figures 3 and 4). (B) T3 occurs on the valley slopes where lacustrine silts rest beneath fine sands. (C) T2 is a well-developed river terrace with fluvial sands covering lacustrine sediments. Three samples (T3-1, −2 and −3) were collected from the fine sands overlying the lacustrine silts of T3. Two samples (T2-1, −2) were collected from the layer of silty sands. (D) Morphology of relict lakes near Changsuo and a 4 m-long drill-core into the lacustrine sediment. Note the location of the borehole in Figure 3.

of Changsuo, it joins two tributaries (Chiblung Chu, Yaru Chu), meets the Ama Drime Massif, then turns southwest and follows the Kharta Fault system. It then cuts across the Himalaya into Nepal and later drains into the Kosi River system, eventually joining the Ganges (Olen *et al.*, 2015). (Note that in the Tibetan language the word ‘tsangpo’ refers a large river rather than any specific river i.e. in English ‘Yarlung Tsangpo’ is equivalent to ‘Yarlung River’. The suffix ‘chu’ is generally used in reference to alpine tributaries.)

The upper reaches of Phung Chu are characterized by wide valleys with braided river channels developed with a relatively low gradient (0.77%), draining a catchment area of *c.* 25 307 km$^2$ (Guan *et al.*, 1984). Alluvial fans are widely developed at mouths of gullies and tributaries on either side of the main river valley. This wide valley becomes a narrow channel in the deeply incised Yö Ri Gorge, where the river suddenly turns to the southwest (highlighted as a yellow rectangle in Figure 1) and flows around the Ama Drime range. Here, the elevation difference from summit to valley floor is over 1400 m. Downstream, the valley topography changes to narrow channels with high gradient slopes, and little fluvial sediment is present within 10 km below the gorge.

The Ama Drime range is bounded by two active normal faults, the Kharta Fault to the west and Dinggye Fault to the east. Spectacular triangular facets, brittle fault planes and cataclasites have been reported and indicate active normal faulting (e.g. Armijo *et al.*, 1986; Zhang and Guo, 2007). Quaternary deposits are offset with an apparent normal sense of displacement along the Nyonno Ri detachment fault, but little is known about its activity in the late Quaternary (e.g. Jessup *et al.*, 2008).

## Geomorphologic Features and Sampling

Lacustrine sediments crop out in the form of terraces on valley slopes along Phung Chu. Three terraces (T3, T2 and T1) can be clearly observed in the field (Figure 2A, the locations for Figures 2A–2D are shown in Figure 1). T3 is *c.* 50 m above riverbed while T2 is *c.* 25 m and T1 $<$ 10 m. Figure 3 shows an enlargement of the red rectangle in Figure 1, where T3 occurs in many segments along Phung Chu (note the risers between terraces are shown in different colors in Figures 3 and 4). T2 is consistently *c.* 25 m lower than T3 at all locations. T1 appears a couple of meters above the riverbed along the main channel. The height differences between terraces were measured using a level. In a number of locations where the river valley is open, fluvio-lacustrine sediments occur in these terraces (Figure 4 shows details for terraces of sampling site, note its location as a black rectangle in Figure 3). For instance, profile A–A′ shows fine sands (2.5 m thick, note its location in Figures 3 and 4B) directly overlying laminated silt layers (2 m thick) near the foot of T3 (28° 35.5′ N, 87° 23.8′ E, field photograph shown in Figure 2B). The lacustrine silt beds dip gently towards the river. A unit of silty sand at T2 is covered by a thin layer of poorly sorted sand and granular gravel; the latter regarded as slope wash or alluvial sediment. Beneath a silty sand layer (~0.2 m thick) lies a thick layer of sand ($>$1.4 m thick, Figure 2C). T1 in this transect consists of sand and granular gravel. On the flat surface of T2 near Changsuo, several small streams run across the terrace and a remnant lake still exists. A 4 m-long drill-core into the T2 near Changsuo reveals a thick layer ($>$2.6 m thick) of clayey silt, suggesting stable lacustrine conditions (Figure 2D). An exposure of lacustrine sediment was found at the mouth of a gully near Changsuo where a $>$ 10 m thickness of continuous well-bedded, lacustrine silt was observed. Several sand dunes occur above lacustrine silts at the east of Changsuo (Figure 1).

The lithostratigraphy of these terraces shows that laterally continuous silt and clay sediments (typical lacustrine deposits) are overlain by silty sand (usually shallow water deposits), with the latter being covered by sand and poorly sorted gravel (slope wash sediments). As such they represent different stages of the lake development. The sedimentary sequences associated with these terraces thus indicate a transition from a relatively deep water lacustrine environment to shallow water lakeshore and

 

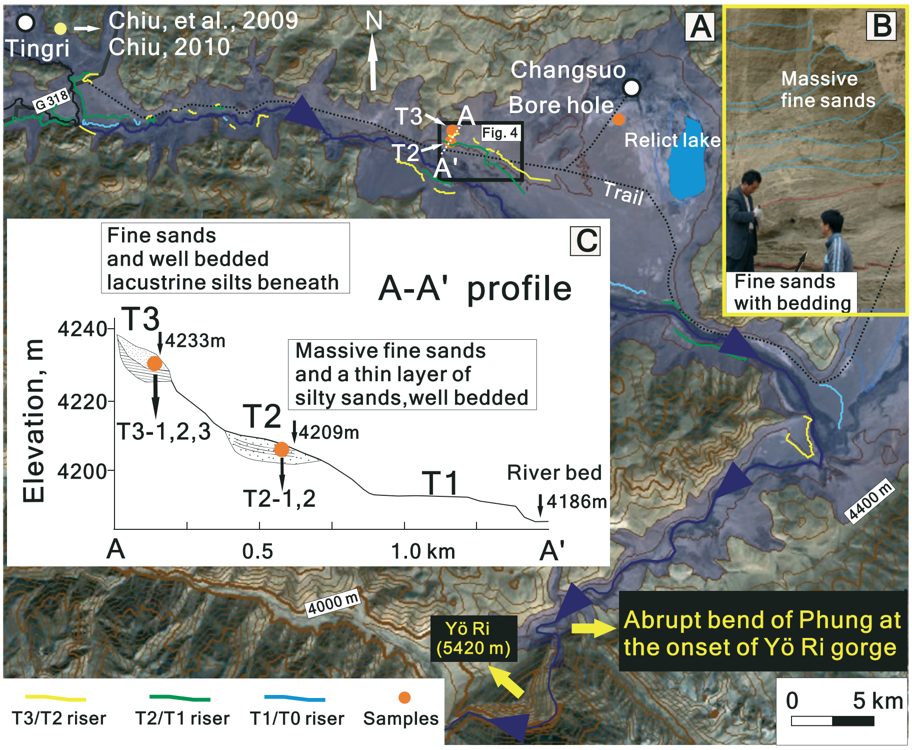


**Figure 3.** (A) Locations of sampling sites and their sedimentological features. Note the risers between terraces are shown in different colors. At some locations, a sub-T1 terrace appears and this is marked by light blue lines. (B) The inset figure (upper right) shows presence of the highest fluvio-lacustrine sediment near New Tingri, at an elevation of about 4400 m a.s.l. (Chiu *et al.*, 2009; Chiu, 2010). (C) Profile A–A′ shows three clearly recognizable terraces.

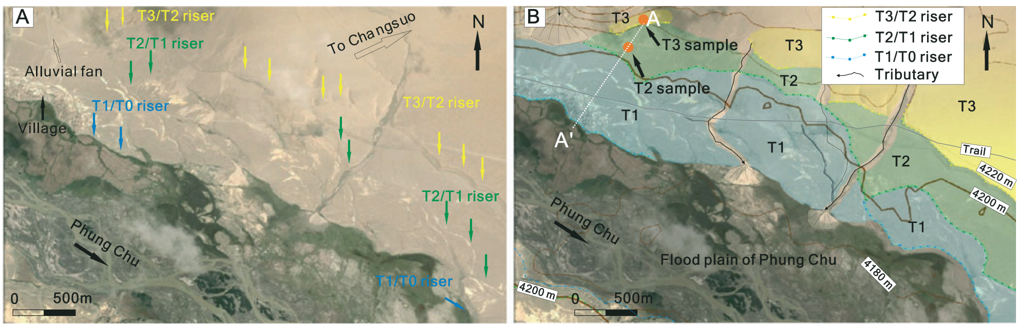


**Figure 4.** The distribution of fluvio-lacustrine sediments along the river course of Phung Chu. (A) Satellite image, note the risers between terraces are shown in different colors. (B) Geomorphology interpretation and three terraces (T3, T2 and T1). Note the location of A–A′ profile from which samples were taken. The contour line of 20-m interval is generated from the Shuttle Radar Topography Mission (SRTM) data (~90-m horizontal resolution).

finally hill slope conditions, implying a process of lake level drop. The lacustrine silt beds dip gently towards the river, suggesting that original terraces could have been tilted by on-going neotectonic activity. Fluvial sediments that overlie the lacustrine silts indicate the likelihood that the palaeo-shorelines have been modified by subsequent fluvial incisions.

In order to determine the time at which the terraces formed, sediment samples were taken for OSL dating from a cleaned cliff-face of the terraces (Figures 2 and 3). For T3, three samples were collected from the foot of T3 from the fine sands just above the well-bedded lacustrine silt layers (28° 35.55′ N, 87° 23.81′ E, Figure 2B, T3-1, −2, −3). Sample T3-2 and T3-3 have a same burial depth of ~3.1 m while the burial depth for T3-1 is about 2.5 m (Figure 2B). For T2, two samples were collected from the silty sands, 0.6 m from its surface (28° 35.38′ N, 87° 23.68′ E, Figure 2C). The burial age of these samples gives an age estimate for termination of lacustrine sedimentation after which the lake level began to drop and fluvial conditions were established.

## Luminescence Dating

### Sample preparation and OSL dating instruments

Under subdued red light conditions, samples were treated by a series of physical and chemical procedures to separate quartz grains for OSL dating (Aitken, 1998). Raw samples were removed from tubes with each end cut away to measure water content and dose rate. Next, 10% hydrochloric acid (HCl) and 20% hydrogen peroxide ($H_2O_2$) were used to remove carbonates and organic materials, respectively. After dry sieving and density separation, quartz grains (125–150 $\mu$m) were separated using sodium polytungstate heavy liquid (with densities between 2.62–2.75 g/cm$^3$). These grains were etched in 40% hydrofluoric acid (90 minutes) to dissolve feldspar grains. Then 10% HCl was used to remove fluorides. The remaining quartz grains were then dried and mounted on aluminum discs (10 mm in diameter) with silicone oil as an adhesive for equivalent dose ($D_e$) measurement. Small aliquots were used all throughout the measurement process (100–300 grains on each aliquot).

OSL signals were measured in the Luminescence Dating Laboratory of the University of Hong Kong, using an automated Risø TL/OSL reader (model DA-20), equipped with a $^{90}Sr/^{90}Y$ beta source (0.125 Gy/s on aluminum discs) as the irradiation source. Blue light-emitting diodes (LEDs) (470 ± 30 nm) were used for optical stimulation for quartz grains. Infrared LEDs (875 ± 80 nm) were used as stimulation light source to check feldspar contamination (60 °C for 100 seconds). OSL signals were detected through two 3-mm-thick Hoya U-340 filters.

## Measuring the equivalent dose ($D_e$)

The single-aliquot regenerative-dose (SAR) protocol (Murray and Wintle, 2000; Wintle and Murray, 2006) was applied to determine the $D_e$. To determine the best preheat temperature, preheat plateau tests were conducted on two samples (T3-1 and T2-1, Figure 5G). From 180 °C to 300 °C with 20 °C increments, $D_e$ values of six aliquots were measured under each preheat temperature. A preheat plateau between 220 and 260 °C was obtained. The $D_e$ values for sample T3-1 exhibit dependence on the preheating temperature, especially for temperatures exceeding 260 °C. Thus, the preheating condition of 240 °C (10 seconds) was used throughout the measurement process. Each measurement comprises preheating (240 °C, 10 seconds), OSL measurement (125 °C, 100 seconds), test dose OSL measurement and other cycles with different regenerative doses. A cut-heat to 200 °C was used prior to the test dose OSL measurements. After sensitivity correction, $D_e$ values were obtained by comparing the natural signal with the signals from different regenerative doses (Figure 5F). 40–60 aliquots were measured for each sample.

The recycling ratio and dose recovery test were used to test the reliability of SAR for our samples (Murray and Wintle, 2000; Wintle and Murray, 2006). Aliquots with a recycling ratio falling outside the range of 1.0 ± 0.1 were discarded in $D_e$ determination. Dose recovery tests were conducted using T3-1 and T2-1. During dose recovery tests, natural signals (24 aliquots) were first bleached by blue light at 125 °C for 100 seconds, followed by a beta dose close to their natural $D_e$ values (150 Gy for T3-1 and 20 Gy for T2-1). SAR protocol was then conducted to measure the value of given dose. Among the 24 aliquots measured, 21 aliquots were adopted for T3-1 and 22 for T2-1. The results show that the ratios of measured dose to a given dose are in the range of 1.0 ± 0.1 (0.97 ± 0.04 for T3-1 and 0.92 ± 0.02 for T2-1), confirming the reliability of the SAR protocol for our samples (see details in Supporting

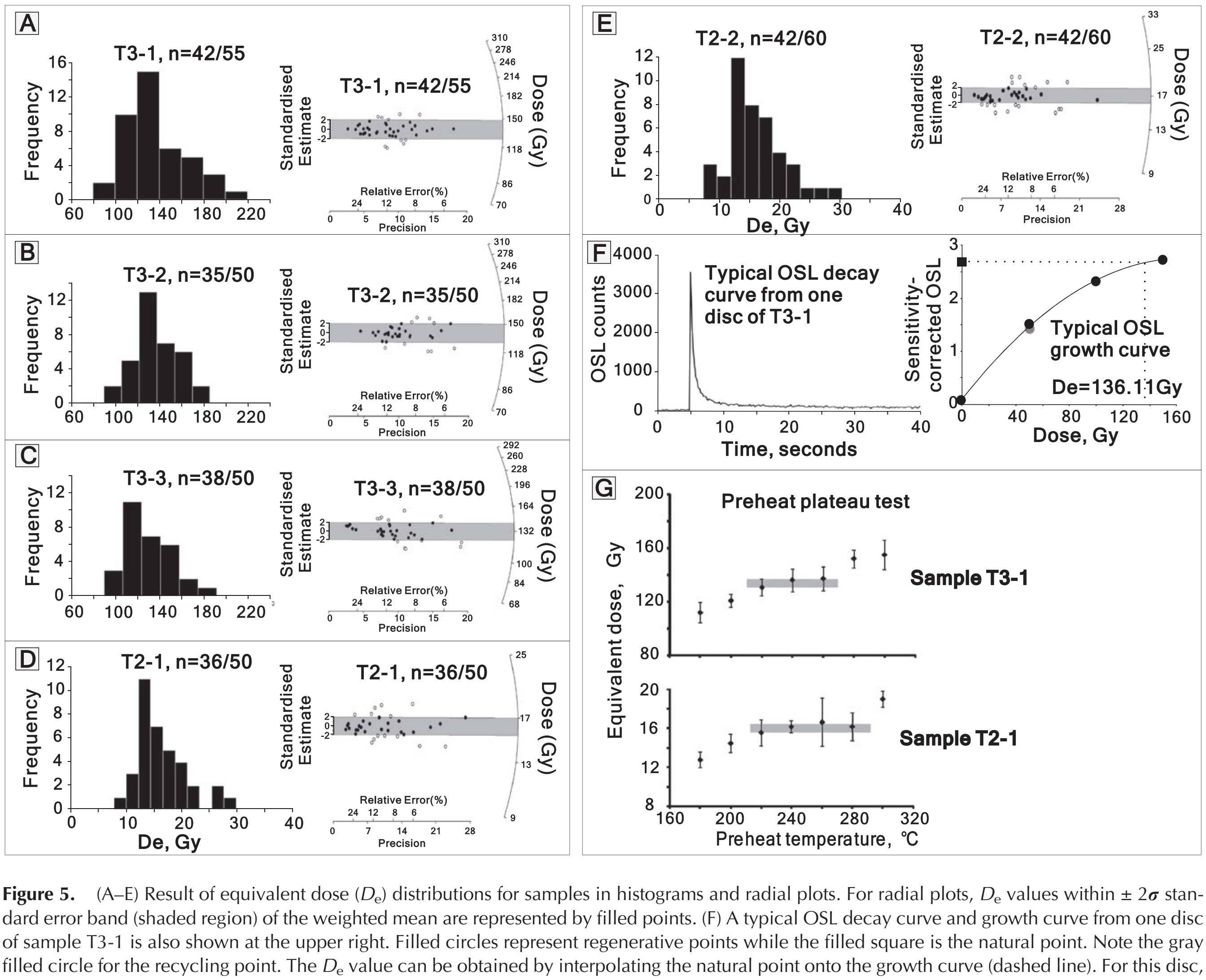


**Figure 5.** (A–E) Result of equivalent dose ($D_e$) distributions for samples in histograms and radial plots. For radial plots, $D_e$ values within ± 2$\sigma$ standard error band (shaded region) of the weighted mean are represented by filled points. (F) A typical OSL decay curve and growth curve from one disc of sample T3-1 is also shown at the upper right. Filled circles represent regenerative points while the filled square is the natural point. Note the gray filled circle for the recycling point. The $D_e$ value can be obtained by interpolating the natural point onto the growth curve (dashed line). For this disc, the $D_e$ value is about 136.11 ± 12.56 Gy. Aliquots adopted for $D_e$ analysis is shown as the total number of aliquots that have been measured ($n$ = 42/55 means that 55 aliquots were measured and 42 of them pass the various tests). (G) Results of preheat plateau tests for samples T3-1 and T2-1.

Information). Recuperation tests were also carried out to monitor possible charge transfer by checking signals from the regenerative point that have received zero irradiation dose. The recuperation ratios for most aliquots are < 5%, for instance, the average recuperation values are 4.60%, 3.76% and 4.63% for T3-1, T3-2 and T3-3, respectively. Feldspar contamination was determined by measuring infrared stimulated luminescence (IRSL) signals (60 °C for 100 seconds). We note that besides this method, some other features can also be used to assess the presence of feldspar, for instance by checking the shape of the 110 °C TL peak (Li *et al.*, 2002). During our measurement any aliquots from which feldspar signals were detected were abandoned.

### Measuring the annual dose

The environmental dose rate contributed from uranium (U) and thorium (Th) decay series was measured by thick source alpha counting technique. The results of alpha counting rates were converted into $\beta$ and $\gamma$ dose rates (Aitken, 1998). Analytical Axios X-ray fluorescence (XRF) spectrometry on fused glass discs was used to determine the potassium content, with the analytical precision estimated to be ±1% (relative standard deviation, RSD). Water content was estimated at 5 ± 2% based on previous studies from the plateau (e.g. Chen *et al.*, 2013b) and laboratory measurement (determined from the loss of sample weights before and after drying at 105 °C in an oven, see details in Supporting Information). Cosmic ray contribution was calculated based on the burial depth of samples and geomagnetic altitude of studying site (Prescott and Hutton, 1994).

### Equivalent dose ($D_e$) distributions

To check whether samples were sufficiently bleached prior to deposition, $D_e$ distributions were investigated using histogram and radial plots. Since all our measurements are based on small aliquots (100–300 grains per aliquot), and most of the OSL signals are usually from only a small fraction of grains (e.g. Duller *et al.*, 2000), the $D_e$ distribution could provide useful information to check whether the OSL signal of the sediment is well reset prior to deposition. Some earlier studies from the Tibetan Plateau have reported that lacustrine sediments such as well-sorted pure sands commonly show OSL signals that are well reset at the time of burial (e.g. Chen *et al.*, 2013b). All the samples in this study show strongly concentrated $D_e$ distributions (Figures 5A–5E). Taking T3-1 as an example, its $D_e$ values show a normal distribution and a tight symmetric peak, suggesting that the residual signals were generally fully bleached prior to deposition. T3-2, −3 and T2-1, −2 also show similar type of $D_e$ distributions, confirming that these samples were bleached sufficiently prior to their burial. The OSL dating results are summarized in Table I. To better assess bleaching conditions from statistical analysis of $D_e$ values, a Central Age Model was applied to calculate the over-dispersion values (Galbraith *et al.*, 1999). The results further suggest it is unlikely that studied samples have the problem of partial bleaching (see details in Supporting Information).

## Results and Discussion

### Possible extent of the palaeo-lake

The location of fluvio-lacustrine sediments provides useful evidence that reveals past lake levels. Notably, however, profiles investigated in this study are relatively limited. Based on the presence of fluvio-lacustrine sediment, the possible extent of this palaeo-lake is roughly estimated. The thick (2 m) laminated silt layers of T3 suggest a stable deep-water environment. A 4.5 m-long profile of massive fine sands and bedded loamy sands has been reported and these sediments occur at about 4400 m a.s.l. near New Tingri (Chiu *et al.*, 2009; Chiu, 2010) (see inset in Figure 3). This suggests that the lake level could have equaled or exceeded this elevation. If taking this elevation as a rough estimate of lake level and using digital elevation model (DEM) data analysis (Shuttle Radar Topography Mission data [SRTM], ~90-m horizontal resolution), a possible extent of this palaeo-lake can be determined (shown as dark blue area in Figure 1). Using this estimation, the palaeo-lake could have covered an area of over 2500 $km^2$, extending 200 km E–W and 80 km N–S, and with a maximum water depth > 200 m. This area is more than twice the size of Nam Co, the largest lake in Tibet at present. It should be noted that the field sites investigated in this study are relatively limited given the large coverage of this dammed-lake and further studies are needed to confirm the extent of the lake and its highest water level.

The terraces investigated in this study dip gently towards the river, suggesting that original terraces could have been tilted or eroded. Such deformation could have been induced by seismic activity due to earthquake shaking (liquefaction and fluidization of sediment layers under the influence of intense earthquake vibrations) or folding due to slumping and landslide (destabilization of a slope due to seismicity as materials upon a steep hillside fall or slide and impact the dammed-lake floor) (e.g. Greb and Dever, 2002; Wang *et al.*, 2011). For instance, similar deformation has been reported from Diexi dammed-lake study in the Minjiang River, on the eastern margin of the Tibetan Plateau (Wang *et al.*, 2011). The tilted terraces in this study thus suggest the possible occurrence of seismicity, i.e. these terraces might have been seismically-modified after their

**Table I.** Optical dating results for fluvio-lacustrine sediment in Tingri

| | Samples | Alpha counting rate[1] | Potassium content[2] (%) | Water content (%) | Cosmic ray[3] (Gy/ka) | Equivalent dose (Gy) | Dose rate (Gy/ka) | Age (ka) |
|---|---|---|---|---|---|---|---|---|
| T3 | T3-1 | 18.79±0.27 | 2.11 | 5±2 | 0.285 | 137.53±4.24 | 4.82±0.19 | 28.53±1.43 |
| | T3-2 | 16.45±0.26 | 2.07 | 5±2 | 0.264 | 137.50±3.52 | 4.44±0.17 | 30.95±1.45 |
| | T3-3 | 15.77±0.25 | 2.17 | 5±2 | 0.264 | 132.41±6.07 | 4.44±0.18 | 29.80±1.80 |
| T2 | T2-1 | 15.70±0.24 | 2.05 | 5±2 | 0.368 | 16.15±0.74 | 4.43±0.17 | 3.65±0.22 |
| | T2-2 | 15.87±0.27 | 2.07 | 5±2 | 0.368 | 17.17±0.74 | 4.47±0.17 | 3.84±0.22 |

Note: Sample T3-1 has an elevation of 4233 m a.s.l., while T3-2 and T3-3 is 0.5 m lower. Sample T2-1 and T2-2 has an elevation of 4209 m. The river level of Phung Chu at A–A' profile is about 4186 m. The burial depth of these samples is shown in Figures 2B and 2C.
[1]The alpha counting rate is for a 42-mm-diameter ZnS screen and is given in units of counts per kilosecond.
[2]The error for the X-ray fluorescence (XRF) spectrometry analyses are estimated to be ± 2% (relative).
[3]The error for the cosmic rays dose rate is estimated at ± 0.02 Gy/ka.

formation. This interpretation implies that seismic events are active controls for landform change in this region, i.e. they have the potential to influence lake evolution. The tilted terraces also suggest that the estimated extent for the palaeo-lake may not reflect the true size due to uncertainty of terrace location and elevation, because the recovered palaeo-lake is based on modern topography and DEM data.

## Drainage history

Along Phung Chu, the elevation of T3, T2 and T1 descends slightly towards the lower reaches, but in general a consistent height difference is maintained between individual terraces as well as with the riverbed. The declining elevation of T3 towards the lower reaches is possibly caused by the natural downstream gradient of the river. The consistent height difference from T3 to the riverbed (*c.* 50 m) at various locations along Phung Chu, however, suggests that T3 is formed by river incision into pre-existing lacustrine sediment, as they are controlled by the same strength of river down-cutting after lake drainage. Thus, they maintain a consistent height difference to the riverbed after that incision event. T2 is consistently *c.* 25 m above the riverbed along Phung Chu, suggesting a similar situation to that of T3. This stratigraphy of the terraces suggests that they formed by fluvial incision.

The three samples collected from T3 yield a consistent age broadly around 30 ka, and two samples from T2 yield an age around 3.7 ka (Table I). It should be noted that the dated fluvio-lacustrine sediments were formed during a lake period, and were then exposed by fluvial incision after the lake drainage. These ages for samples from the terrace surfaces thus indicate times that predate, or are close to, the onset of lake drainage events, i.e. a minimum age estimate for the timing of lake drainage. In other words, a lake formed before 30 ka, followed by two drainage events that took place soon after 30 ka and 3.7 ka respectively. One possible scenario is that the lake drained around 30 ka and river incision formed T3, then the channel was blocked again, formed a new dammed-lake until about 3.7 ka, when the second drainage event happened and formed T2. This suggests that Phung Chu could have been repeatedly blocked in the late Quaternary. Another explanation is that the first drainage 30 ka ago was partial, and caused the lake level to drop by *c.* 25 m. Fluvio-lacustrine sedimentation was maintained after the first drainage event until the second drainage event took place at 3.7 ka, when the lake was totally drained. This could imply that a dammed lake may have been present for ~26 ka (Figure 6).

Exactly when the Phung Chu palaeo-lake first formed remains unknown. Our results presented here only suggest that the lake should have formed well before 30 ka. Further studies are needed to confirm this. Moreover, a catastrophic flood event could have occurred when the lake drained, leading to large-scale erosion and rapid landform change. If so, flood deposits like large boulders up to several meters in size should occur in areas downstream of the gorge. Similar boulders have been reported to indicate a catastrophic flood for the partial drainage of Pangong Tso in western Tibet (Dortch *et al.*, 2011).

## Possible controls on the dammed lake

Possible explanations for blocking Phung Chu need to be considered. Firstly, ice damming and moraine deposition during glacial advance could block such a river. This is an important mechanism for river blockage and dammed-lake formation, especially for regions of the southeast Tibetan Plateau where moraine deposits commonly develop during a glacial period. Such glacial dams in adjacent regions on the Tibetan Plateau have also been reported as typical reason for river blockage, with links to river incision and topography development on the plateau (e.g. Korup and Montgomery, 2008; Liu *et al.*, 2015). For instance, based on radiocarbon dating of lacustrine and alluvial terraces, it is reported that two dammed lakes (832 $km^3$ and 80 $km^3$ of water) immediately upstream of the Yarlung Tsangpo gorge formed in the early Holocene and possibly resulted in megafloods with catastrophic failure of glacial dams (e.g. Montgomery *et al.*, 2004). From satellite survey images, two possible moraine ridges are located about 2.5 km upstream of the Yö Ri gorge (Figure 7A). These ridges are ~400 m above river level and suggest that moraine deposition is a potential candidate for the damming of Phung Chu. Few glacier studies have been reported from this region. At this stage we consider that glacial damming is a possible cause for formation of Phung Chu lake. However, further studies of sediment distribution and characteristics and the chronology of glacial deposits in this region are needed to test this hypothesis.

Landslides are also a common cause of river blockage (e.g. Korup *et al.*, 2010). Near the Yö Ri gorge, Phung Chu does not run straight along the Kharta Fault, but deviates around Mount Yö Ri via the Yö Ri gorge (lower middle of Figure 3, also see Figure 7). The high-gradient slope topography near Mount Yö Ri further suggests it is an ideal location for landsliding

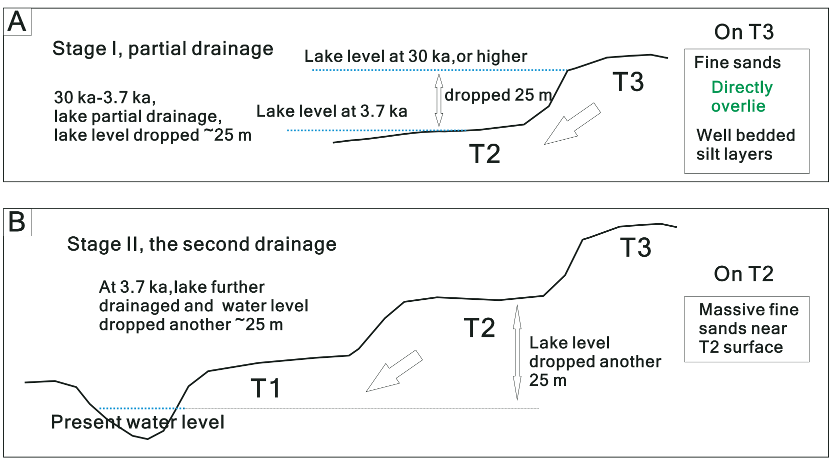


**Figure 6.** A reconstructed evolutionary history of the Phung Chu palaeo-lake, if according to our interpretation the lake went through a two-phase drainage. (A) The first drainage after 30 ka was partial and water level dropped ~25 m. (B) The lake was totally drained after second drainage event took place after 3.7 ka.

 

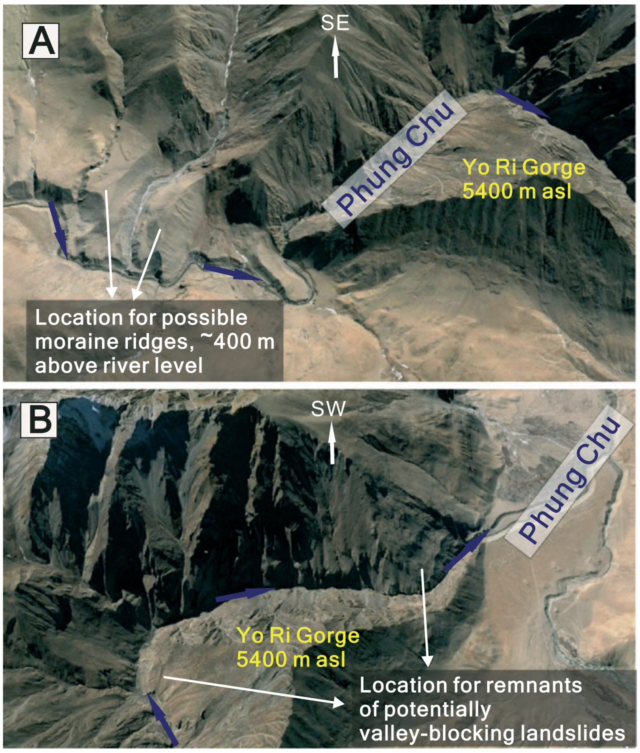


**Figure 7.** Locations for possible blockage of Phung Chu. (A) Possible moraine ridges. (B) Potential remnants of landslides. Base satellite imagery is from Google Earth.

and river damming. Upstream from the Yö Ri gorge, fluvio-lacustrine sediment and terraces are abundant, while no lacustrine sediment is seen in the gorge. Two possible remnants of potentially valley-blocking landslides within the Yö Ri gorge can be observed clearly (Figure 7B), suggesting that landsliding is also a possible cause for blocking of Phung Chu.

Landslides can be triggered by a variety of causes including heavy precipitation and seismic events. Seismic activity is a common mechanism for triggering landslides in tectonically active regions. Similar dammed lake evolutions in the marginal regions of the Tibetan Plateau have also been reported (e.g. Zhang *et al.*, 2011; Chen *et al.*, 2013a). The formation of modern landslide-dammed lakes by this mechanism is also recorded during the 2008 Wenchuan Earthquake (Parker *et al.*, 2011; Yuan *et al.*, 2013). Local lithology, secondary compaction, caliche cementation from mineralized water and weathering processes are key factors controlling the stability of a landslide blockage as well as the life span of landslide-dammed lakes (Weidinger, 2011). If the lake drainage is a two-phase event as our explanation suggests, then a Phung Chu landslide-dammed lake could have been present for ~26 ka. Such long life spans for landslide- and glacier-triggered dams have also been reported (e.g. Deline and Orombelli, 2005; Korup *et al.*, 2006). For instance, glacier blockage of the Shyok River is reported to have lasted for more than 100 ka in the Karakoram (Scherler *et al.*, 2014). However, rainfall induced-landslides can form dammed lakes but such lakes usually last for only a short interval as the dam is easily re-opened by subsequent erosion when water level exceeds the dam (e.g. Guan and Chen, 1980; Li *et al.*, 2009). Moreover, the tilted terraces imply the possible occurrence of seismicity and thus strengthen the possibility for seismic events that triggered the blockage of Phung Chu. Given that the active Kharta Fault is associated with the on-going tectonic activity related to the uplift and denudation of the Ama Drime Massif (e.g. Jessup *et al.*, 2008), we suggest that a seismic event is the most likely cause of landsliding and blockage of Phung Chu, rather than a heavy precipitation-induced landslide.

In summary, combining channel deviation for Phung Chu near the Yö Ri gorge, the high-gradient slope topography in the gorge and the active Kharta Fault, we propose that a landslide triggered by a seismic event is a likely reason for the formation of the Phung Chu dammed lake. However, moraine deposits suggest that glacial damming cannot be excluded as a possible cause of blockage of Phung Chu. This study suggests these controls play a key role in landform evolution in marginal regions of the Tibetan Plateau in the late Quaternary.

## Conclusions

Based on investigation of the large palaeo-dammed-lake along Phung Chu, this study provides new information regarding late Quaternary landscape evolution along the southern margin of the Tibetan Plateau. This investigation has produced new results on the spatial distribution and sedimentary characteristics of the two fluvio-lacustrine terraces and their significance in regards to palaeoseismicity and potential geo-hazards posed by modern analogues in mountainous regions. The timings of two phases of lake drainage were constrained by applying OSL methods to sediment samples collected from the terraces. Results show that (1) a palaeo-dammed-lake of over 2500 km$^2$ in size formed before 30 ka ago, and it could have reached a lake level of 4400 m a.s.l.; (2) the first lake drainage occurred after 30 ka and formed T3 at 50 m height from the present river level, whilst a second drainage event happened after 3.7 ka and formed T2 at 25 m height from the present river level; (3) these two drainage events may have been independent of one another and Phung Chu may have been repeatedly blocked in the late Quaternary. However, it is also possible that the first drainage was partial and the lake remained until a second drainage took place after 3.7 ka.

Given the distribution of the fluvio-lacustrine terraces, active normal faults in this region (particularly the Kharta Fault) and high gradient slopes downstream from where Phung Chu enters the Yö Ri gorge, seismically induced landsliding is regarded as the most likely cause for drainage blockage and ensuing formation of the dammed-lake, although glacial damming of Phung Chu is also possible. The formation of this large dammed lake may have influenced local climate as the lake surface area was as large as 2500 km$^2$. Although the palaeo-climatic hypothesis needs to be tested by further research, this study has provided evidence for linking seismic activity to fluvio-lacustrine landscape processes and possible palaeo-climatic change.

The tectonically active Tibetan Plateau is an ideal region for generating dammed-lakes, particularly in its eastern, southern and western margins, which are the source of several of the world's largest rivers. Catastrophic drainages of these dammed-lakes may cause severe floods, which place up to one billion people living in the Indian sub-continent, southeast Asia and China at risk of significant geo-hazards. From an example in the most tectonically active region, this study adds to general knowledge of the landscape process mechanisms associated with the development and drainage of dammed-lakes. This type of knowledge is critically important for geo-hazard risk assessment and natural disaster mitigation. Further work is needed to obtain more information on this special landform not only for understanding geomorphic evolution but also for modeling natural disasters.

*Acknowledgements*—The two anonymous reviewers and editors are appreciated for their constructive comments and detailed recommendations, with special thanks given to the second reviewer for providing detailed satellite survey images. This work is supported by a research grant (HKU700109) from the Research Grant Council, Hong Kong SAR, National Nature Science Foundation of China (41402150) and a grant from GIG-CAS (SKLIG-RC-13-02).

## References

Aitken MJ. 1998. An Introduction to Optical Dating. Oxford University Press: Oxford; 267.

Armijo R, Tapponnier P, Mercier JL, Han T-L. 1986. Quaternary extension in southern Tibet-field observations and tectonic implications. *Journal of Geophysical Research* **91**: 13803–13872.

Burchfiel BC, Chen Z, Hodges KV, Liu Y, Royden LH, Deng C, Xu J. 1992. The South Tibetan Detachment System, Himalayan Orogen: extension contemporaneous with and parallel to shortening in a collisional mountain belt. *Geological Society of America Special Paper* **269**: 1–41.

Chen J, Dai F, Lv T, Cui Z. 2013a. Holocene landslide-dammed lake deposits in the Upper Jinsha River, SE Tibetan Plateau and their ages. *Quaternary International* **298**: 107–113.

Chen Y, Zong Y, Li B, Li S-H, Aitchison JCA. 2013b. Shrinking lakes in Tibet linked to the weakening Asian monsoon in the past 8.2 ka. *Quaternary Research* **80**: 189–198.

Chiu H. 2010. Sedimentology and Geomorphology of Modern and Relict Lake Systems in Tibet, PhD Thesis. Faculty of Science, University of Hong Kong, Hong Kong.

Chiu H, Switzer A, Zong Y, Aitchison JC. 2009. Geomorphic and sedimentological evidence of a drained lake system and associated environmental change Tingri, Tibet, China. *Geological Society of America Abstracts with Programs Volume* **41**: 170.

Costa JE, Schuster RL. 1988. The formation and failure of natural dams. *Geological Society of America Bulletin* **100**: 1054–1068.

Costa JE, Schuster RL. 1991. *Documented Historical Landslide Dams from Around the World*, US Geological Survey Open-File Report 91. Reston, VA: US Geological Survey; 486.

Dai F, Lee C, Deng J, Tham LG. 2005. The 1786 earthquake-triggered landslide dam and subsequent dam-break flood on the Dadu River, southwestern China. *Geomorphology* **65**: 205–221.

Deline P, Orombelli G. 2005. Glacier fluctuations in the western Alps during the Neoglacial, as indicated by the Miage morainic amphitheatre (Mont Blanc massif, Italy). *Boreas* **34**: 456–467.

Dortch JM, Owen LA, Caffee MW, Kamp U. 2011. Catastrophic partial drainage of Pangong Tso, northern India and Tibet. *Geomorphology* **125**: 109–121.

Duller GAT, Botter-Jensen L, Murray AS. 2000. Optical dating of single sand-sized grains of quartz: sources of variability. *Radiation Measurement* **32**: 453–457.

Fan X, Rossiter DG, van Westen CJ, Xu Q, Gorum T. 2014. Empirical prediction of coseismic landslide dam formation. *Earth Surface Process and Landforms* **39**: 1913–1926.

Galbraith RF, Roberts RG, Laslett GM, Yoshida H, Olley JM. 1999. Optical dating of single and multiple grains of quartz from Jinmium rock shelter, northern Australia: Part 1, Experimental design and statistical models. *Archaeometry* **41**: 339–364.

Greb SF, Dever GR. 2002. Critical evaluation of possible seismites: examples from the carboniferous of the Appalachian basin. *Geological Society of America Special Papers* **359**: 109–125.

Guan Z, Chen C. 1980. Water resources for Tibetan rivers. *Resources Science* **2**: 25–35.

Guan Z, Chen C, Ou Y, Fan Y, Zhang Y, Chen Z, Bao S, Zu Y, He X, Zhang M. 1984. Tibetan River and Lakes. Scientific Press: Beijing; 238.

Hanson MA, Lian OB, Clague JJ. 2012. The sequence and timing of large late Pleistocene floods from glacial Lake Missoula. *Quaternary Science Reviews* **31**: 67–81.

Heron AM. 1922. Geological Results of the Mount Everest Expedition, 1921. *The Geographical Journal* **59**: 418–431.

Jessup MJ, Newell DL, Cottle JM, Berger AL, Spotila JA. 2008. Orogen-parallel extension and exhumation enhanced by denudation in the trans-Himalayan Arun River gorge, Ama Drime Massif, Tibet-Nepal. *Geology* **36**: 587–590.

Keefer DK. 1984. Landslides caused by earthquakes. *Geological Society of America Bulletin* **95**: 406–421.

Keefer DK. 1994. The importance of earthquake-induced landslides to long-term slope erosion and slope-failure hazards in seismically active regions. *Geomorphology* **10**: 265–284.

Kong P, Granger DE, Wu F-Y, Caffee MW, Wang Y-J, Zhao X-T, Zheng Y. 2009. Cosmogenic nuclide burial ages and provenance of the Xigeda paleo-lake: implications for evolution of the Middle Yangtze River. *Earth and Planetary Science Letters* **278**: 131–141.

Korup O, Densmore AL, Schlunegger F. 2010. The role of landslides in mountain range evolution. *Geomorphology* **120**: 77–90.

Korup O, Montgomery DR. 2008. Tibetan plateau river incision inhibited by glacial stabilization of the Tsangpo gorge. *Nature* **455**: 786–790.

Korup O, Strom AL, Weidinger JT. 2006. Fluvial response to large rock–slope failures: examples from the Himalayas, the Tien Shan, and the Southern Alps in New Zealand. *Geomorphology* **78**: 3–21.

Leloup PH, Maheo G, Arnaud N, Kali E, Boutonnet E, Liu D, Liu X, Li H. 2010. The South Tibet detachment shear zone in the Dinggye area Time constraints on extrusion models of the Himalayas. *Earth and Planetary Science Letters* **292**: 1–16.

Li C, Zhang Y, Du W. 2009. Investigation and risk removal of the landslide-dammed lake of Yigong, Tibet. *Science and Technology Information* **13**: 719–720.

Li S-H, Sun J, Zhao H. 2002. Optical dating of dune sands in the northeastern deserts of China. *Palaeogeography, Palaeoclimatology, Palaeoecology* **181**: 419–429.

Liu WM, Lai ZP, Hu KH, Ge YG, Cui P, Zhang XG, Liu F. 2015. Age and extent of a giant glacial-dammed lake at Yarlung Tsangpo gorge in the Tibetan Plateau. *Geomorphology* **246**: 370–376.

Mangerud J, Astakhov VI, Murray A, Svendsen JI. 2001. The chronology of a large ice-dammed lake and the Barents-Kara Ice Sheet advances, northern Russia. *Global and Planetary Change* **31**: 321–336.

McColl ST. 2012. Paraglacial rock–slope stability. *Geomorphology* **153–154**: 1–16.

Montgomery DR, Hallet B, Liu Y, Finnegan N, Anders A, Gillespie A, Greenberg HM. 2004. Evidence for Holocene megafloods down the Tsangpo River gorge, southeastern Tibet. *Quaternary Research* **62**: 201–207.

Murray AS, Wintle AG. 2000. Luminescence dating of quartz using an improved single-aliquot regenerative-dose protocol. *Radiation Measurements* **32**: 57–73.

Nagelisen J, Moore JR, Vockenhuber C, Ivy-Ochs S. 2015. Post-glacial rock avalanches in the Obersee Valley, Glarner Alps, Switzerland. *Geomorphology* **238**: 94–111.

Olen SM, Bookhagen B, Hoffmann B, Sachse D, Adhikari DP, Strecker MR. 2015. Understanding erosion rates in the Himalayan orogen: a case study from the Arun Valley. *Journal of Geophysical Research: Earth Surface* **120**(10): 2080–2102. DOI. 10.1002/2014JF003410

Parker RN, Densmore AL, Rosser NJ, de Michele M, Li Y, Huang R, Whadcoat S, Petley DN. 2011. Mass wasting triggered by the 2008 Wenchuan earthquake is greater than orogenic growth. *Nature Geoscience* **4**: 449–452.

Prescott JR, Hutton JT. 1994. Cosmic ray contribution to dose rates for luminescence and ESR dating: large depths and long-term time variations. *Radiation Measurements* **23**: 497–500.

Scherler D, Munack H, Mey J, Eugster P, Wittmann H, Codilean AT, Kubik P, Strecker MR. 2014. Ice dams, outburst floods, and glacial incision at the western margin of the Tibetan Plateau: A >100 k.y. chronology from the Shyok Valley, Karakoram. *Geological Society of America Bulletin* **126**: 738–758.

Wager LR. 1937. The Arun River drainage pattern and the rise of the Himalaya. *The Geographical Journal* **89**: 239–250.

Wang L, Yang L, Wang X, Duan L. 2005. Discovery of huge ancient dammed lake on upstream of Minjiang River in Sichuan, China. *Journal of Chengdu University of Technology* **32**: 1–11.

Wang P, Zhang B, Qiu W, Wang J. 2011. Soft-sediment deformation structures from the Diexi paleo-dammed lakes in the upper reaches of the Minjiang River, east Tibet. *Journal of Asian Earth Sciences* **40**: 865–872.

Weidinger JT. 2011. Stability and life span of landslide dams in the Himalayas (India, Nepal) and the Qin Ling Mountains (China). In Natural and Artificial Rockslide Dams, Volume 133: Lecture Notes in Earth Sciences, Evans SG, Hermanns RL, Strom A, Scarascia-Mugnozza G (eds). Springer: Berlin; 243–277.

Wintle AG, Murray AS. 2006. A review of quartz optically stimulated luminescence characteristics and their relevance in single-aliquot regeneration dating protocols. *Radiation Measurement* **41**: 369–391.

Yin Y, Wang F, Sun P. 2009. Landslide hazards triggered by the 2008 Wenchuan earthquake, Sichuan, China. *Landslides* **6**: 139–151.

Yuan R-M, Deng Q-H, Cunningham D, Xu C, Xu X-W, Chang C-P. 2013. Density distribution of landslides triggered by the 2008 Wenchuan Earthquake and their relationships to peak ground acceleration. *Bulletin of the Seismological Society of America* **103**: 2344–2355.

Zhang J, Guo L. 2007. Structure and geochronology of the southern Xainza-Dinggye rift and its relationship to the south Tibetan detachment system. *Journal of Asian Earth Sciences* **29**: 722–736.

Zhang Y, Zhao X, Lan H, Xiong T. 2011. A Pleistocene landslide-dammed lake, Jinsha River, Yunnan, China. *Quaternary International* **233**: 72–80.

Zhu S, Wu Z-H, Zhao X-T, Xiao K-Y. 2013. Glacial dammed lakes in the Tsangpo River during late Pleistocene, southeastern Tibet. *Quaternary International* **298**: 114–122.

## SUPPORTING INFORMATION

Supporting information can be found in the on-line version of this article.